

Trapped Vortex in Ground Effect

Darwin L. Garcia* and Joseph Katz†

San Diego State University, San Diego, California 92182

The effects of vortices trapped between a flat plate and a ground plane were studied in a wind-tunnel experiment. The flat plate was mounted parallel to the ground to represent the lower surface of a generic road vehicle. Rectangular vortex generators, much taller than the local boundary layer, were mounted on the flat plate to generate streamwise vortices between the plate and the ground plane. The main variables investigated were the ground clearance and vortex generator orientation, both influencing the trapped vortex strength. The experimental data indicate that considerable aerodynamic loads can be created with such vortex generators, even when the flat plate is parallel to the ground. Ground proximity had a significant effect on the aerodynamic loads, particularly on the lift, which increased rapidly with reduced ground clearance.

Nomenclature

\mathcal{AR}	=	d/a , vortex-generator spacing aspect ratio
a	=	vortex generator height (1 in.; 25 mm)
C_D	=	drag coefficient
C_L	=	lift coefficient
C_M	=	pitching-moment coefficient
c	=	plate chord (30 in.; 762 mm)
d	=	lateral spacing between vortex generators
h	=	ground clearance
L/D	=	lift/drag ratio
l	=	vortex-generator length (6 in.; 152 mm)
M	=	pitching moment (positive direction defined in Fig. 2)
V_∞	=	freestream speed
w	=	plate width (16 in.; 406 mm)
β	=	vortex-generator yaw angle

Introduction

THE principle of increasing fluid dynamic loads by creating strong vortices near solid surfaces existed in nature long before attempts were made to understand its mechanics. It is natural, therefore, that vorticity is frequently used to explain an airfoil's lift, which is often called "bound vorticity" (to separate it from "unbound" vortices found in wakes). Consequently, augmentation of the fluid dynamic loads (e.g., an airfoil's lift) by adding unbound (or trapped) vortices is a logical extension to the "more vorticity more lift" principle. Indeed, the potential benefits of the trapped-vortex model were investigated by Rossow,² but in this study the practical problem of stabilizing the vortex above a stationary airfoil remained unresolved. In his later work^{3,4} Rossow proposed vertical fences to stabilize the trapped vortex, but this solution remains suitable to basic laboratory work only and still impractical to flying aircraft. Although this difficulty of stabilizing a two-dimensional trapped vortex limits its engineering applicability, the three-dimensional trapped-vortex case can be made stable, as indicated in Refs. 4 and 5. Buchholz and Tso⁵ demonstrated that the leading-edge vortices of highly swept wings can be captured, and by doing so they can clearly increase the lift at the smaller angle-of-attack range (at which range the usual leading-edge vortices are too weak or nonexistent). In conclusion, it seems that the trapped vortex is a viable principle for

lift augmentation, but its practical utilization is still in the proof-of-concept stage. Apart from this narrow range of highly swept wings⁵ at very low angles of attack, practical levels of lift augmentation in the presence of a trapped vortex were not demonstrated. The only situation where significant (momentary) lift augmentations were reported is in the case of transient flowfields created by insects¹ or by impulsively started airfoils.⁶

Ground vehicles, contrary to aircraft, move close to the ground, and their incidence relative to the freestream falls into the small angle-of-attack (or zero incidence) category. The utilization of this type of vortex lift, therefore, becomes quite attractive. For example, such vortices when trapped beneath a moving automobile and the ground can increase the vehicle's negative lift (downforce). This aerodynamic downforce is often exploited by race-car designers in order to increase tire adhesion and vehicle's high-speed performance. Early efforts to evaluate the effect of ground proximity on the downforce, created by downward-pointing swept wings (applicable to race cars), were reported by Katz and Levin.⁷ In this work the leading-edge vortices were created by the swept-wing surface, which had to be oriented at least 10 deg (negative) relative to the freestream. To apply the trapped-vortex principle to a ground vehicle whose lower surface is usually parallel to the ground, additional vortex generators (swept from the top view) must be used. This approach allows the vortex strength to be almost independent of vehicle incidence, and their position can be fixed by trapping devices (e.g., fences, such as proposed by Rossow³). This particular problem of longitudinal vortices, but now with ground effect, is a clear descendant of the earlier trapped-vortex ideas. However, in spite of this inherent similarity this particular problem was not studied in the past and will be the focus of the present study.

Experimental Apparatus

The effect of ground proximity on the trapped vortices was investigated by the generic experimental setup depicted in Figs. 1 and 2. The vehicle's lower surface was represented by a rectangular flat plate, with small vortex generators (VG) added to create the streamwise vortices (Fig. 1). These VGs are much larger than those used on airplane wings,⁸ where the height of the VG is on the order of the local boundary layer. Also, their length is much greater than in airplane applications, and the current size was dictated by Indy-car geometry.⁹ Furthermore, such race cars will have a curved (and not flat) underbody; however, results presented in Ref. 9 clearly show that the important features were captured by this simplified experiment. As Fig 2 indicates, the plate (representing the vehicle's lower surface) was mounted onto the six-component balance by three struts. The forward two struts were 12 in. (300 mm) apart, and only one is visible in the side view presented in Fig. 2. The ground plane (thin flat plate) could move up and down by actuators placed outside the test section to vary the ground clearance. The advantage of this inverted setup (e.g., the ground is above the model) was that the metric flat-plate model was mounted directly to the balance

Received 19 April 2002; revision received 19 November 2002; accepted for publication 3 December 2002. Copyright © 2003 by the American Institute of Aeronautics and Astronautics, Inc. All rights reserved. Copies of this paper may be made for personal or internal use, on condition that the copier pay the \$10.00 per-copy fee to the Copyright Clearance Center, Inc., 222 Rosewood Drive, Danvers, MA 01923; include the code 0001-1452/03 \$10.00 in correspondence with the CCC.

*Graduate Student, Department of Aerospace Engineering, 5500 Campanile Drive. Member AIAA.

†Professor, Department of Aerospace Engineering, 5500 Campanile Drive. Associate Fellow AIAA.

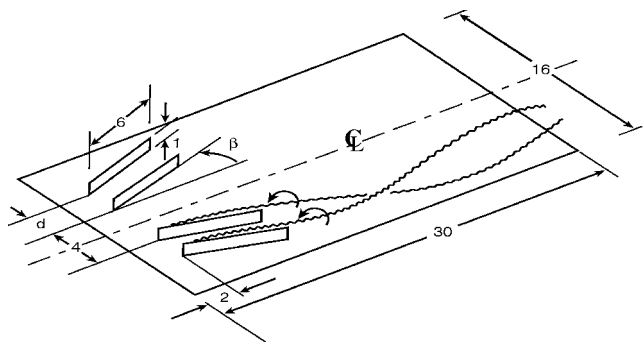


Fig. 1 Flat-plate model with the vortex generators (dimensions in inches). Note schematic description of vortex roll up at larger ground clearance values.

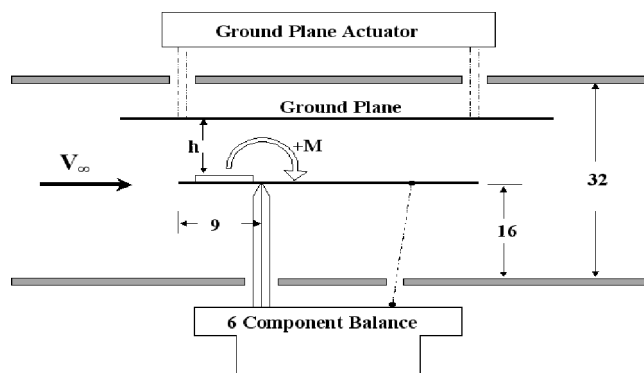


Fig. 2 Flat plate with the vortex generators, as mounted in the wind tunnel. Note that the model is mounted on the three struts upside down (and pitch angle was kept at 0 deg) while the ground plane could move down toward the stationary model. Dimensions are in inches, and M indicates the positive direction of the pitching moment.

(which is placed under the wind tunnel) and only the nonmetric ground plane was moving (up and down). Because of the preliminary nature of this investigation, a moving-ground simulation (e.g., by a rolling belt) was not used; however, future studies could focus on matching the ground-plane speed with the freestream speed for better simulation of an actual vehicle on the ground.

Wind-tunnel blockage was small (less than 1%), and the effect of the ground-plane installation (on the blockage ratio) was negligible too. Two rectangular vortex generators per each side of the symmetry line (in Fig. 1) were used, following Rossow's^{3,4} observation that at least two fences are required to stabilize the vortex. Of course more and different shape VGs (e.g., triangular) could have been tested, but the objective of this work was to document the most basic features of the trapped-vortex flowfield near the ground. The spanwise and chordwise position and the yaw angle of the VG were adjustable, but their vertical orientation was fixed (e.g., at 90 deg to the flat plate). For the data presented here the separation distance between the leading edge of the inner VG was kept constant (at a total of 4 in.; 101 mm), and it was yawed about this point (positive β defined into the outward direction; see Fig. 1). The test section height of the San Diego State University low-speed wind tunnel is 32 in. (813 mm), and its width is 45 in. (1143 mm). Freestream speed throughout these tests was set at 120 mph (53.60 m/s), and turbulence levels in the test section were about 2%. Additional dimensions of the model and its position in the test section are depicted in Figs. 1 and 2. Because of the sharp edges of the VGs, it is assumed that Reynolds-number effects are less pronounced, and results of this vortex flow experiment are scalable. Based on the flat-plate length the test Reynolds number was 2.7×10^6 . Accuracy of the six-component balance was about ± 0.004 for C_L , ± 0.002 for C_D , and ± 0.0003 for C_M . The model plan-view area (30×16 in.; 0.31 m^2) and its length (30 in.; 762 mm) were used as reference quantities for the preceding nondimensional coefficients. In this setup positive lift is upward, and positive moment is into the nose-up direction, as depicted in Fig. 2 (and so in terms of ground vehicles the lift measured here is really downforce).

Also, the ground clearance was measured between the upper tip of the VG and the ground plane above it (Fig. 2), whereas the pitch axis was located at 30% of the plate chord (where the front struts axis meets the flat plate (Fig. 2).

Results

A vortex generator, such as that depicted in Fig. 1, is expected to create suction force on the plate along the vortex core extending behind the VG itself. Therefore, aerodynamic loads can be created on the flat plate without changing its incidence from the zero angle-of-attack position (and this feature is important for ground vehicles). It appears that more VGs will create more aerodynamic loads, but at least two (per side) are needed for this preliminary investigation (so that effects such as lateral spacing could be studied). A large volume of experimental data with this setup is reported in Ref. 10, but only those necessary to summarize the major trends will be presented here. For example, variables such as VG angle β or lateral spacing are the most basic and therefore will be presented first.

The effects of VGs sideslip angle β on the measured aerodynamic loads are presented in Figs. 3–5. For this case the two sets of VGs were set parallel to each other (on each side), and their angle relative to the freestream was varied between 10 and 30 deg. (Of course the 0-deg case resulted in no aerodynamic lift, but the C_D of the model was about 0.031.) Varying VG angle to the opposite direction (negative β) was tested and did not produce the desirable lift; therefore, those results are not reported here. (One way to look at this effect is to consider that VGs at positive β will direct the flow outside of the gap between the plate and the ground, whereas negative β will have an opposite, detrimental effect on lift.) Returning to Fig. 3, the data clearly show that the larger VG incidence resulted in stronger vortices and more lift, which effect, in general, increases with reduced ground clearance. The drag data presented in Fig. 4 follow similar trends with maximum lift/drag

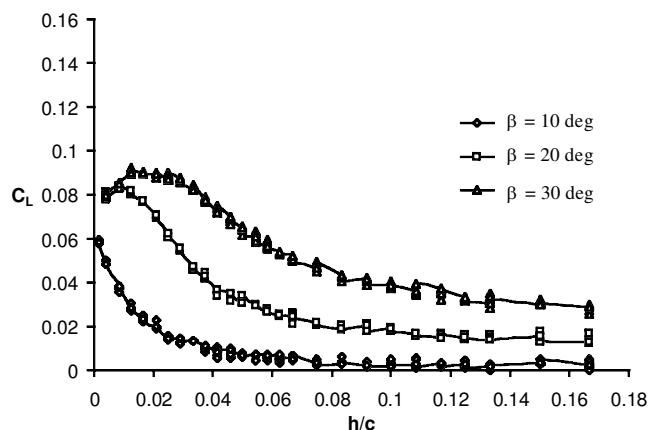


Fig. 3 Effect of VG yaw angle on the flat-plate lift. Spacing between the two parallel VGs on each side was kept constant ($d = 1.0$ in.; 25 mm).

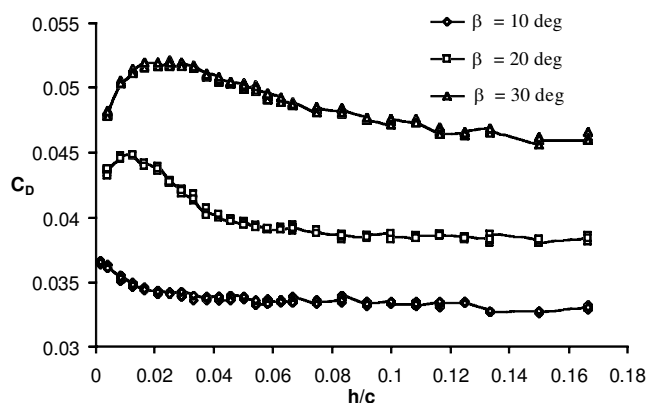


Fig. 4 Effect of VG yaw angle on the flat-plate drag. Spacing between the two parallel VGs on each side was kept constant ($d = 1.0$ in.; 25 mm).

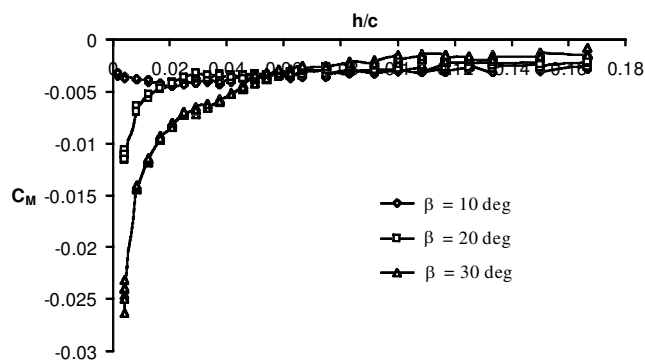


Fig. 5 Effect of VG yaw angle on the flat-plate pitching moment. Spacing between the two parallel VGs on each side was kept constant ($d = 1.0$ in.; 25 mm).

ratios measured within the 1.2–1.6 range. At this point some properties of the leading-edge vortices can be revisited (and the vortices created by the VGs can be viewed as leading-edge vortices from a slender thin wing). Polhamus¹¹ showed that such leading-edge vortices tend to burst at larger incidence angles (vortex breakdown), an effect which also reduces their lift. (He also provided a diagram for delta wings summarizing vortex burst position vs angle of attack.) In a later work Levin and Katz¹² speculated that vortex breakdown-vs-incidence relation for rectangular surfaces is quite similar to that presented by Polhamus for the triangular surfaces. By following this rationale, it appears that at higher sideslip angles β the vortex breakdown is closer to the VG's trailing edge (explaining the peak in lift at lower h/c for increased β angles in Fig. 3). At this point the proximity of the preceding vortex burst to the VG can be discussed. For example, the negative sign of the pitching moment (in Fig. 5), even for the high ground clearance values, indicates that the vortex core (suction) effect takes place behind the VGs. Note that the pitching moment is measured relative to the 30% chord of the plate, a position clearly behind the VG trailing edge. Also, as the ground plane approaches the model the suction force intensifies, particularly at the aft section creating a larger nose-down moment, and this additional effect can be explained by the unwinding of the vortex roll up (of the two neighboring VGs as shown in Fig. 1).

On and off the surface flow visualizations (using tufts) revealed a quite complex vortex phenomena, even with this simple VG geometry. It appears that at the larger ground clearance values the two vortices from the two VGs (from each side) interact, lifting and rolling the outer one (see schematic description in Fig. 1). As ground clearance is reduced, these vortices are forced closer to the surface, also gradually untwisting themselves at the same time, which explains the larger negative moment and lift. (So both lift and moment effects are dominated by the suction force behind the VGs.) As the ground moves even closer, vortex breakdown moves forward (particularly for $\beta > 30$ deg), and a maximum in the lift is detected. This is in agreement with the observation that at the larger VG angle β this maximum in lift is reached at a larger ground clearance. It appears too that at the lowest test angle (e.g., $\beta = 10$ deg) vortex breakdown did not play a significant role, and the lift monotonically increases almost down to zero ground clearance. This is further reinforced by the pitching-moment diagram (Fig. 5), where for the $\beta = 10$ deg case the VG vortices behind the trailing edge are less affected by the ground proximity, balancing the loads about the moment center (hence almost no change in pitching moment). Further speculation about the effect of ground proximity calls for examining the limiting condition of $h/c = 0$. However, because in this case the flow between the VGs and the ground plane is blocked no vortex will form, and the vortex wake-induced lift will be lost. This condition was not tested, and at the lowest ground clearance value of $h/c = 0.0042$ the vortex effect was still significant.

The effect of lateral spacing is demonstrated in Figs. 6–8. For scaling purposes the frontal area aspect ratio (between the VGs) can be defined as ($AR = \text{VG lateral spacing}/\text{VG height}$, or d/a). The lift data presented in Fig. 6 seem to increase with the increase in AR . Clearly, when $AR = 2$ [e.g., $d = 2$ in. (51 mm) in Fig. 1, because VG

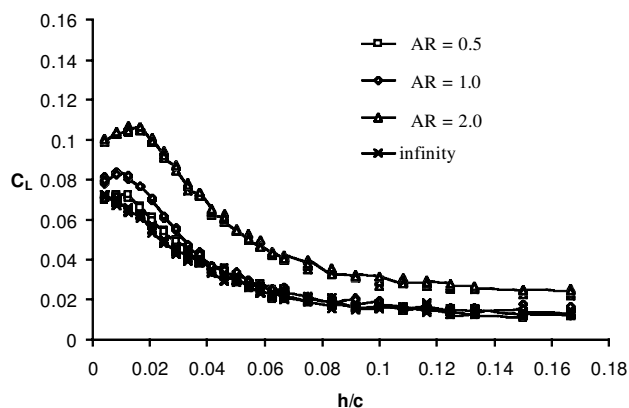


Fig. 6 Effect of VG lateral spacing on the flat-plate lift (parallel VGs, $\beta = 20$ deg).

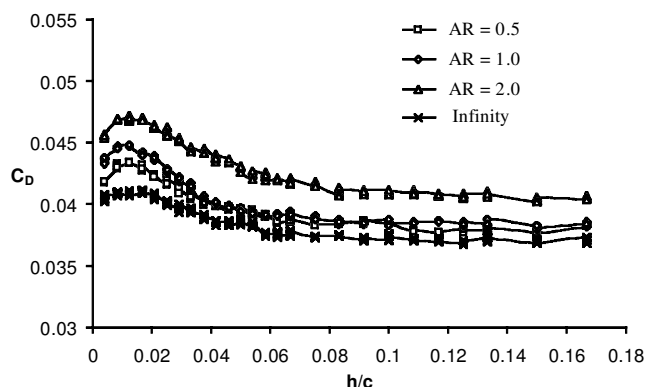


Fig. 7 Effect of VG lateral spacing on the plate drag (parallel VGs, $\beta = 20$ deg).

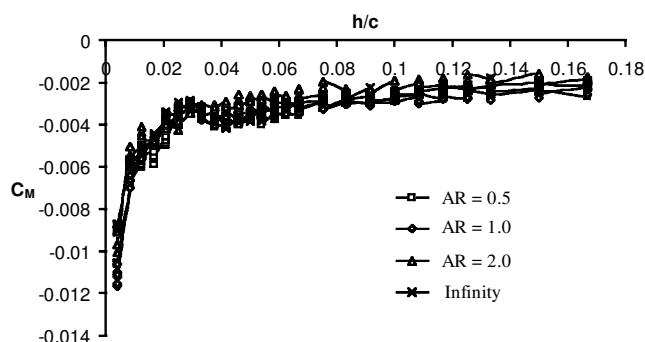


Fig. 8 Effect of VG lateral spacing on the flat-plate pitching moment (parallel VGs, $\beta = 20$ deg).

height is $a = 1$ in. (25 mm)], then lift increases significantly throughout all of the ground clearance values tested. For comparison, the outer VG was removed from each side, representing an infinite spacing (condition $AR = \infty$). It appears that the lift of a single VG (on each side) is comparable to the lift of the two at their closest spanwise spacing (e.g., at $AR = 0.5$), proving that vortex interaction is not always favorable. The drag coefficient in Fig. 7 follows similar trends to that of the lift coefficient in Fig. 6. When comparing Figs. 6 and 7 with Figs. 3 and 4, respectively, it appears that in Figs. 6 and 7 the maximum loads occur at almost the same ground clearance value as for the $\beta = 20$ deg case in Figs. 3 and 4 (because the yaw angle of the VGs is the same). For a similar reason the variation of the pitching moment (in Fig. 8) is not affected by the spanwise positioning of the VGs, compared to the strong effect of varying the yaw angle. Also, the single VG case and the largest AR case do not differ (from this aspect), and the aerodynamic loads are almost doubled with the two VGs. This might suggest that the second VG is not needed to “trap” the vortex, and each VG is able to create

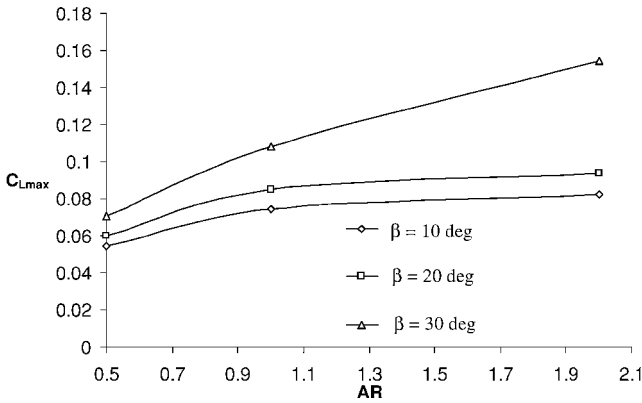


Fig. 9 Maximum lift coefficient vs lateral spacing of parallel vortex generators.

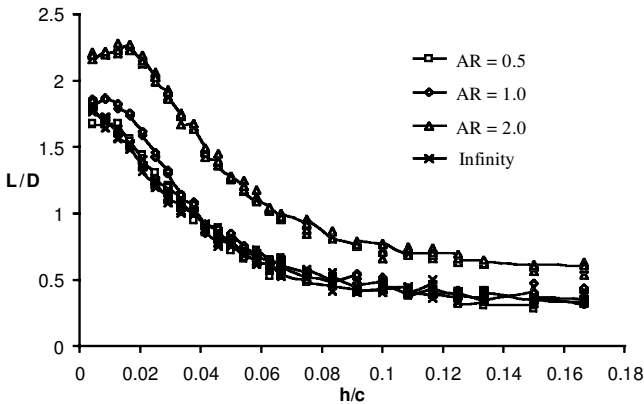


Fig. 10 Lift-to-drag ratio vs ground clearance for several lateral spacing (parallel VGs, $\beta = 20$ deg).

a stable vortex of its own (contrary to Ref. 4), and the interaction between the vortices is more of “vortex roll-up” type.

A summary of the maximum lift vs AR (parallel VGs) is depicted in Fig. 9. The trend, as pointed out, is toward increased lift with the larger spacing. Values larger than $AR = 2$ were not tested because they appear impractical for such generic ground vehicle applications (e.g., race cars). Also, as mentioned, less interaction between the VGs appears to produce more aerodynamic loads; again, indicating that the second VG is not needed to stabilize (or trap) the vortex from the first VG.

Figure 10 demonstrates the typical lift/drag ratios obtainable with this setup, based on the data in Figs. 6 and 7. In general, practical vehicle clearances are less than the height of the VG (e.g., VG height/ c of 0.0333), and Fig. 10 indicates that the L/D ratio is significantly larger than one in this range. The wider VG spacing also produced the larger L/D ratios, and the general trends in this figure are very close to the results for the lift in Fig. 6. Also, the maximum values of L/D are important, and the data point toward ratios of over two, which could be surpassed with some modifications (see Ref. 10 and the following examples).

One of the ideas tested was to set the VGs in a diverging configuration to allow more space for the forming vortices between the “fences.” Indeed this approach resulted in larger lift values, and the corresponding data are presented in Figs. 11–13. In this case the inner VGs were set at $\beta = 10$, while the outer VGs yaw angle varied at $\beta = 10, 20$, and 30 deg, respectively (spacing was $AR = 2$). The lift data, when compared to similar data (e.g., in Fig. 3 or 6) measured with the parallel VG configuration, clearly prove that larger lift values were obtained here. The drag data in Fig. 12 show values similar to those in Fig. 4 or 7, suggesting that L/D values for this case are higher (indeed L/D_{\max} is slightly over 2.2 for this case). The pitching moment data here (Fig. 13) are in the same range as before, apart from the $\beta = 30$ deg case, where the trend at high ground clearance values is somewhat different. It is possible that

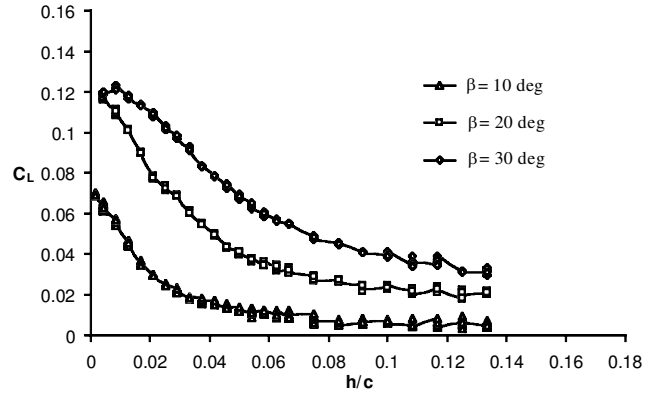


Fig. 11 Effect of varying yaw angle between the two adjacent VGs on the flat-plate lift. β on figure represents orientation of outer VG (inner VG at $\beta = 10$ deg and $AR = 2$).

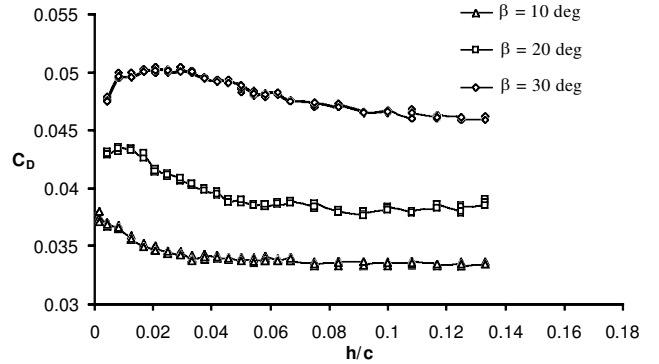


Fig. 12 Effect of varying yaw angle between the two adjacent VGs on the flat-plate drag. β on figure represents orientation of outer VG (inner VG at $\beta = 10$ deg and $AR = 2$).

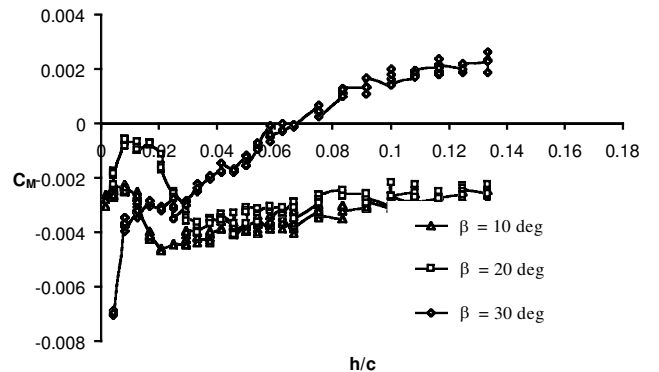


Fig. 13 Effect of varying yaw angle between the two adjacent VGs on the flat-plate pitching moment. β on figure represents orientation of outer VG (inner VG at $\beta = 10$ deg and $AR = 2$).

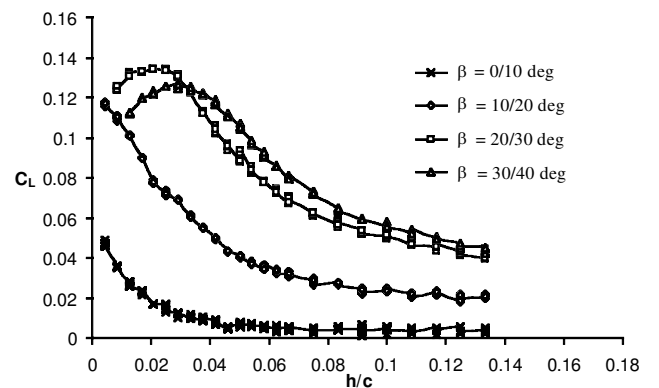


Fig. 14 Effect of varying yaw angle of the pair of VGs (set 10 deg apart and $AR = 2$) on the flat-plate lift.

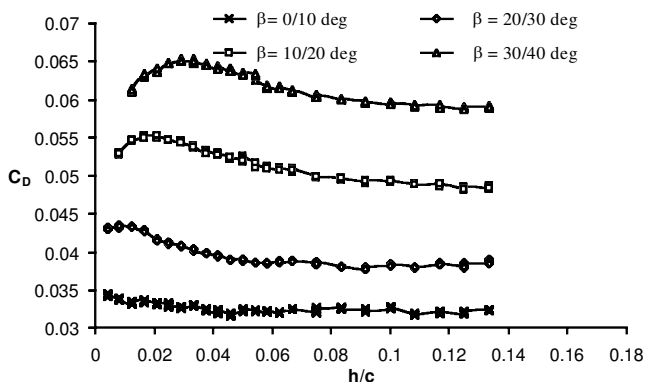


Fig. 15 Effect of varying yaw angle of the pair of VGs (set 10 deg apart and $AR = 2$) on the flat-plate drag.

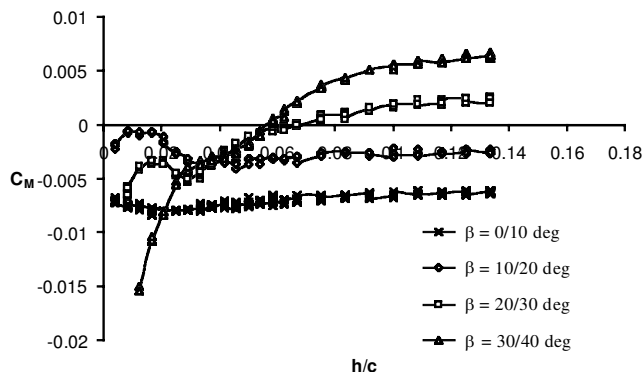


Fig. 16 Effect of varying yaw angle of the pair of VGs (set 10 deg apart and $AR = 2$) on the flat-plate pitching moment.

the stronger (outer) vortex is higher (above the plate, because of the roll up described in Fig. 1) and its effect on the plate will increase with reduced ground clearance. In the other two cases (e.g., $\beta = 10$ and 20 deg) the initial trend is of moderate increase (absolute) of negative moment with the reduction in ground clearance, similar to the preceding data. However, in this case of larger spacing ($AR = 2$) when ground clearance is reduced below $h/c = 0.02$, the moment curve trend is reversed for $\beta = 10$ and 20 deg (possibly because of a more complex vortex interaction).

The last "basic" variation is similar to the case of rotating the sets of the VGs outward, but now (compared to Figs. 3–5) there is a diverging angle difference of 10 deg between the fences. Those data are presented in Figs. 14–16 (and spacing remains at $AR = 2$). It appears that because of vortex breakdown in the case of $\beta = 40$ deg the resulting lift (caused by that VG) is reduced, leading to the conclusion that VG yaw angle should be kept below 40 deg. Again, this diverging geometry of the VGs resulted in higher levels of lift than the parallel configurations presented earlier (e.g., Figs. 3–5). For example, with the inner VG at $\beta = 20$ deg and the outer at $\beta = 30$ deg, respectively, the largest values of lift were observed (and the largest L/D_{\max} is over 2.2 , again). Drag values were comparable

with the preceding data apart from the $\beta = 30/40$ deg case, where the vortex burst of the outer VGs is the reason for the significant increase in the drag coefficient.

The pitching moment in this case (Fig. 16), compared to Fig. 13, exhibits a wider spread as a result of the just-mentioned complex interaction between vortex roll up and burst, for the larger VG angles of $\beta = 30$ to 40 deg. In case of the $30/40$ -deg data, and at the higher ground clearance values, actually a positive moment was measured, indicating that most of the load (in the lifting direction) is concentrated near the VGs and not behind the pitch axis (e.g., less suction from the far vortex wakes).

Conclusions

Vortex generators when used between the ground and a road vehicle's lower surface can create sizeable aerodynamic loads, even at the (vehicle's) zero-angle-of-attack condition. These loads usually increase as ground clearance is reduced. It appears that for an efficient design the vortex generators should not be spaced too closely to each other because their interaction appears to reduce the aerodynamic loads. Also, vortex breakdown behind the VGs depends primarily on their own incidence relative to the freestream, much like in the case of an isolated rectangular plate at the same angle of attack. The "double fence" model for trapping and stabilizing the vortices, as originates from two-dimensional models, is not necessarily applicable in the three-dimensional case. Also the complex interaction between the VGs vortices and the ground, involving vortex roll up and breakdown, warrants future numerical and flow-visualization studies (and additional investigations with rolling ground effects).

References

- 1Weis-Fogh, T., "Unusual Mechanisms for the Generation of Lift in Flying Animals," *Scientific American*, Vol. 233, No. 5, 1975, pp. 80–87.
- 2Rossow, V. J., "Lift Enhancement by an Externally Trapped Vortex," *Journal of Aircraft*, Vol. 15, No. 9, 1978, pp. 618–625.
- 3Rossow, V. J., "Two-Fence Concept for Efficient Trapping of Vortices on Airfoils," *Journal of Aircraft*, Vol. 29, No. 5, 1992, pp. 847–855.
- 4Rossow, V. J., "Aerodynamics of Airfoils with Vortex Trapped by Two Spanwise Fences," *Journal of Aircraft*, Vol. 31, No. 1, 1994, pp. 146–153.
- 5Buchholz, M. D., and Tso, J., "Lift Augmentation on Delta Wing with Leading-Edge Fences and Gurney Flap," *Journal of Aircraft*, Vol. 37, No. 6, 2000, pp. 1050–1057.
- 6Katz, J., Yon, S., and Rogers, S. E., "Impulsive Start of a Symmetric Airfoil at High Angle of Attack," *AIAA Journal*, Vol. 34, No. 2, 1996, pp. 225–230.
- 7Katz, J., and Levin, D., "Measurement of Ground Effect for Delta Wings," *Journal of Aircraft*, Vol. 21, No. 6, 1984, pp. 442, 443.
- 8Lin, J. C., Robinson, S. K., McGhee, R. J., and Valarezo, W. O., "Separation Control on High-Lift Airfoils via Micro-Vortex Generators," *Journal of Aircraft*, Vol. 31, No. 6, 1994, pp. 1317–1323.
- 9Katz, J., and Garcia, D., "Aerodynamic Effects of Indy Car Components," Society of Automotive Engineers, Paper 2002-01-3311, Dec. 2002.
- 10Garcia, L. D., "Trapped Vortex in Ground Effect," M.S. Thesis, Dept. of Aerospace Engineering, San Diego State Univ., San Diego, CA, May 2002.
- 11Polhamus, E. C., "Prediction of Vortex Characteristics by a Leading-Edge Suction Analogy," *Journal of Aircraft*, Vol. 8, No. 4, 1971, pp. 193–199.
- 12Levin, D., and Katz, J., "Self Induced Oscillations of Low Aspect Ratio Rectangular Wings," AIAA Paper 90-2811, Aug. 1990; also *Journal of Aircraft*, Vol. 29, No. 4, 1992, pp. 698–702.

J. P. Gore
Associate Editor